RSC Mechanochemistry

ROYAL SOCIETY OF CHEMISTRY

PAPER

View Article Online
View Journal

Cite this: DOI: 10.1039/d5mr00111k

Using piezoelectric mechanochemistry for solvent-free, nonthermal defluorination of perfluoroalkyl substances (PFAS) contained in carbon-based sorbents

Andres F. Prada, * Jaemin Kim, Linduo Zhao, Fangyu Li, Lee Green and John W. Scott

Mechanochemical methods such as ball milling offer a solvent-free and non-thermal approach for PFAS remediation, enabling not just separation but actual destruction of PFAS through defluorination. In this study, we demonstrate that effective PFAS defluorination using ball milling critically depends on the presence of a co-milling catalyst, in this case piezoelectric catalysts such as boron nitride (BN), which showed the highest performance among other tested piezoelectric materials. While BN has already proven effective for defluorination of pure PFAS compounds, PFAS in sediments, and aqueous film-forming foam (AFFF), prior studies have been limited by the small amounts of PFAS they can treat inside another medium. To overcome these limitations, we present as an alternative the coupling of BN with activated carbon as a pre-concentration medium for PFAS. By leveraging activated carbon's high sorption capacity, we were able to destroy nearly 100 times higher mass of PFOA in less than one-third of the time compared to previous studies on sediments or AFFF. These results suggest that the design of larger-scale ball milling systems for PFAS destruction should incorporate the use of high-capacity sorbents to concentrate contaminants, thus destroying higher amounts more effectively. While in the case of activated carbon the chances of reusing it after milling are minimal, it could be safely disposed of without the risk of releasing PFAS back into the environment.

Received 5th September 2025
Accepted 15th October 2025

DOI: 10.1039/d5mr00111k

rsc.li/RSCMechanochem

1. Introduction

Per- and polyfluoroalkyl substances (PFAS) are a large class of synthetic organic compounds that have drawn significant attention over the past two decades due to their environmental persistence, potential for bioaccumulation, and toxicity.[1] Among them, perfluorooctanoic acid (PFOA) has been widely used as a precursor in the manufacture of numerous industrial and consumer products, including firefighting foams, fluoropolymers, pesticides, and liquid-repellent textiles.[2] In recognition of its environmental and health risks, PFOA was listed as a persistent organic pollutant under the Stockholm Convention in 2009 and was subsequently banned or severely restricted by international agreement in 2019 (Decision SC-9/12). Despite these regulatory efforts, PFOA remains detectable in various environmental media such as groundwater,[3] drinking water,[4] and landfill leachate.[5] Due to the strength of its carbon–fluorine (C–F) bonds (~485 kJ mol^{-1}),[6] PFOA is highly resistant to degradation, with estimated half-lives of approximately 50 years in water.[7]

To manage PFAS contamination, several technologies have been developed and applied for their physical separation from water, including activated carbon adsorption, anion exchange resins, nanofiltration, reverse osmosis, ozonation, and foam fractionation.[8,9] Some of these methods have achieved over 90% removal efficiency for long-chain PFAS.[10,11] However, there is the potential risk of PFAS release from disposed materials as confirmed from landfill leachate data which show some of the highest PFAS concentrations among environmental and industrial water streams,[12] highlighting the need to destroy PFAS laden in materials prior to their disposal. As a result, there is growing interest in treatment technologies that go beyond separation and focus on the actual destruction of PFAS compounds—specifically, through defluorination.

Incineration has been identified by the U.S. EPA as the only currently viable solution for PFAS destruction,[13] as it is capable of full defluorination of PFAS compounds.[14,15] However, concerns remain regarding the volatilization of shorter-chain PFAS and the potential emission of toxic organic fluorine byproducts or perfluorinated carbons. In response, the U.S. Department of Defense has emphasized that incineration of

Illinois Sustainable Technology Center, Prairie Research Institute, University of Illinois at Urbana-Champaign, 1 Hazelwood Dr., Champaign, IL 61820, USA. E-mail: pradase2@illinois.edu; jaemin@illinois.edu; zhao117@illinois.edu; seanl6@illinois.edu; leegreen@illinois.edu; zhewang@illinois.edu

PFAS-laden materials should only be applied under strictly controlled conditions, following detailed protocols aligned with Clean Air Act requirements.[16] As alternatives, several non-incineration approaches have been developed for treating solid-phase PFAS, including supercritical water oxidation,[17] UV-advanced reduction processes,[18] non-thermal plasma,[19] hydrothermal alkaline treatment,[20] electrochemical oxidation,[21] or mechanochemical degradation.[22] Among these, mechanochemical methods—such as ball milling—offer a promising, solvent-free, and energy-efficient strategy for PFAS destruction in solid matrices, and are increasingly viewed as a more sustainable option.[23]

Mechanochemical degradation of PFAS, particularly using ball milling systems, was first introduced by Zhang *et al.*[24] In their study, various co-milling reagents—including CaO, SiO_2, Fe–SiO_2, NaOH, and KOH—were tested to enhance the defluorination efficiency of solid-phase PFOS and PFOA. Among these, KOH proved to be the most effective, achieving over 90% fluoride recovery after 4 to 8 hours of treatment.[24] Yang *et al.* (2023), however, argued that the high chemical loading required for KOH—exceeding a 20 : 1 weight ratio—posed limitations for practical applications and disposal of treated materials (caustic residues), highlighting the need for more efficient co-milling reagents.[25] They proposed boron nitride (BN) as a promising alternative. BN is a piezoelectric material traditionally used as an electrical insulator due to its wide band gap (~6.0 eV), but it is increasingly regarded as a wide band gap semiconductor.[26] For PFAS treatment, BN's crystalline structure and piezoelectric properties enable the generation of localized electric potentials upon mechanical impact, which can cleave the strong C–F bonds.[25] Yang *et al.* (2023) demonstrated that BN, used at a BN to solid-phase PFAS weight ratio of 5 to1, could mineralize over 90% of pure PFOA and PFOS within 2 to 4 hours, and over 80% of 21 PFAS species detected in 2 grams (g) of sediment samples after 6 to 10 hours of treatment.[25]

Zhu *et al.* (2025) later used similar techniques to destroy up to 2 mg of PFOS adsorbed in different types of anion exchange resins under more than 3 hours of treatment with the assistance of BN as well.[27] Additionally, Yang *et al.* (2025) applied similar principles and parameters to demonstrate complete defluorination of 100 to 1000 μL of undiluted aqueous film-forming foam (AFFF) under ambient conditions, using a combination of boron nitride (BN) and quartz sand (SiO_2).[28] However, a major barrier to further implementation of piezoelectric ball milling strategies is the small scale at which this technology has been developed, suitable only for treating limited quantities of contaminated liquids or solids. To address this, Yang *et al.* (2023) proposed using larger equipment, such as tumbler ball mills, to enable treatment of greater volumes of undiluted AFFF.[28]

Here we demonstrate an alternative, and potentially more practical, approach involving pre-treating contaminated liquids by filtering them through activated carbon, followed by ball milling the PFAS-laden activated carbon. Activated carbon has proven to be an effective sorbent, particularly for long-chain PFAS, with adsorption capacities ranging from 100 to 400 milligrams of PFAS per gram of carbon.[29,30] In their study, Yang *et al.* (2025) worked with AFFF containing a total organic fluorine concentration of 9080 mg L^{-1}.[28] At this concentration, one gram of activated carbon could concentrate PFAS from nearly 50 mL of AFFF, adsorbing up to 400 mg of PFAS, and representing a 50-fold increase in the volume treated using the same ball milling setup and energy input, compared to the direct treatment of only 1 mL. This approach highlights the potential to scale up PFAS remediation of high concentrated solid materials without the need of scaling the equipment or increasing the energy consumption, and offers an alternative to incineration or reactivation practices for PFAS-laden activated carbon.

In this study, we demonstrate the effectiveness of piezoelectric ball milling for mineralizing nearly 90% of PFOA adsorbed onto activated carbon. The high level of defluorination was achieved after just 2 hours of treatment, using the optimized dosage of boron nitride (BN) previously shown to be effective for pure, solid-phase PFAS.[25] By first adsorbing PFAS from aqueous solutions onto activated carbon, this approach lays the groundwork for a simple, scalable, and practical remediation strategy—operable at ambient temperature and pressure, and producing no harmful by-products aside from clean defluorination. Although we found that activated carbon cannot be reused due to a roughly 50% reduction in surface area from repeated mechanical impacts, the high fluoride recovery confirms that the treated carbon can be safely disposed of, mitigating long-term environmental risks.

2. Methods

2.1. Sorption of PFOA into activated carbon

All materials were of analytical grade, procured from commercial sources, and used as received. PFOA ($CF_3(CF_2)_6COOH$, 95%, Sigma-Aldrich) was used for all experiments in amounts of 100 mg. Activated carbon (powder, Darco® G-60, −100 mesh, Sigma-Aldrich) was used in amounts of 1 g, and all co-milling catalysts: boron nitride (BN, powder, ~1 μm, 98%, Sigma-Aldrich), aluminum nitride (AlN, powder, 10 μm, ≥98%, Sigma-Aldrich), or silica (SiO_2, prepared by grinding natural flint stone in-house) were each used at a fixed weight ratio of 5 : 1 relative to the PFOA, corresponding to 500 mg. This catalyst dosage was maintained in both experiments involving pure PFOA and 1 g of PFOA-laden activated carbon, as the adsorbed PFOA content was standardized at 100 mg.

For sorption onto activated carbon, 100 mg of PFOA were dissolved in 100 mL of nanopure water (>18.0 MΩ cm; Labconco Water Pro Plus system, Kansas City, MO, USA) in 125 mL glass vessels. One gram of activated carbon was then added to each vessel. The vessels were sealed with Parafilm and placed on a temperature-controlled reciprocal shaker, operated at 200 rpm and maintained at 25 ± 0.5 °C for 24 hours. After shaking, the vessels were left undisturbed on a countertop to allow the activated carbon to settle. Then, 1 mL of the supernatant was collected from the center of each vessel for PFAS analysis to verify sorption.

PFAS analysis was conducted using a Shimadzu 8050 Ultra High-Performance Liquid Chromatography tandem Mass

Spectrometry (LC-MS/MS) system (Kyoto, Japan). Detection used electrospray ionization (EIS+) and multiple-reaction monitoring (MRM) modes. Prior to each assay, the instrument was calibrated using seven calibration standards made with reference standards obtained from Wellington Laboratories (Guelph, Ontario, Canada), for a detection range of 1–100 parts-per-billion (ppb). Quality control measures included the use of isotope-labeled surrogates and internal standards, as well as continuing calibration blanks, reagent blanks, and independently prepared check standards. Final PFAS concentrations were calculated using the isotope dilution method, which corrects native PFAS levels based on surrogate recoveries. Reported values represent the average of multiple sample preparations and analyses. Associated errors were determined using either the relative percent difference (%RPD) or relative standard deviation (%RSD) across replicate measurements.

2.2. Ball milling

The underlying mechanisms of PFAS destruction by ball milling remained unclear; specifically, whether defluorination is driven primarily by the presence of co-milling catalysts or if other factors, such as mechanical force from ball collisions, friction, or heat generation during milling, also contribute. In the ball milling system used in this study, the force exerted by the milling balls at the specified rotational speed has been previously estimated at approximately 57 N,[25] and the temperatures inside the stainless steel jars can reach around 60 °C after 1 to 8 hours of milling,[28] though higher localized temperatures may occur during the process. In a prior study, Yang *et al.* (2025) performed milling tests (2 and 4 hours) using pure perfluorooctanesulfonic acid (PFOS) without a catalyst and found nearly zero defluorination.[28] To verify this and to expand on the full understanding of our system, we conducted a more comprehensive experiment using pure PFOA, milled without any catalyst for 1 to 4 hours in triplicate.

For the experiments on activated carbon, after sorption, the PFAS-laden activated carbon was collected and dried in an oven at 60 °C overnight prior to ball milling treatment. Once dried, each gram of activated carbon was added along with 500 mg of one of the previously described catalysts and placed into stainless steel jars containing stainless steel balls (100 mL jars, 16 Ø 1.0 cm large balls and 100 Ø 0.6 cm small balls, 160 g in total). Each jar was sealed with a rubber gasket and lid, then clamped into a planetary ball mill (PQ-N04, Across International), which accommodates four jars. All four jars were milled simultaneously for 1 to 4 hours at 580 rpm (Fig. S-1). At this operating speed, the mill consumes 0.14 kWh per hour, as measured using a plug-in power meter. Therefore, the total energy consumption for the milling process ranges from 0.14 to 0.56 kWh, depending on the treatment duration.

After ball milling, the contents of each jar were rinsed with nanopure water into pre-cleaned 200 mL glass beakers. The beakers were previously washed, fired at 450 °C for 4 hours, and triple-rinsed with methanol, toluene, and ammonium hydroxide. A 5 mL aliquot of the rinse water was collected to quantify fluoride ion yielded and thus confirm the cleavage of C–F bonds and, consequently, the defluorination of PFOA. Defluorination efficiency was calculated as the percentage of measured fluoride ions relative to the total fluorine content of the initial PFOA. The instrument used was an ion chromatography system (Dionex ICS-2100, Thermo Scientific, Waltham, MA), calibrated with fluoride reference standards obtained from SPEX CertiPrep (Metuchen, NJ), covering a detection range of 1–100 parts per million (ppm). Fluoride measurement alone may miss partially degraded fluorinated organic compounds, including shorter-chain PFAS or other fluorine-bearing byproducts that retain C–F bonds but are not mineralized.[31]

The milled activated carbon was then dried overnight at 60 °C for subsequent analysis of Brunauer–Emmett–Teller (BET) surface area, scanning electron microscopy (SEM), and energy-dispersive X-ray spectroscopy (EDS). BET surface area measurements were performed using a Micromeritics Gemini VII analyzer (Norcross, GA), based on 11-point adsorption isotherms over a relative pressure (P/P°) range of 0.05–0.3. SEM analysis was conducted using a Hitachi S-4800 High-Resolution SEM (Tokyo, Japan), and elemental characterization *via* EDS was performed using a Shimadzu EDX-7000 Energy-Dispersive X-ray Fluorescence Spectrometer (Tokyo, Japan).

3. Results and discussion

3.1. Defluorination of PFOA adsorbed in activated carbon

Our results confirmed that mechanical factors alone, namely ball collisions, friction, and heat, contributed to only ~1% defluorination (Fig. 1A). In the absence of a catalyst, we observed variability in the defluorination of pure PFOA over time proved by differences in statistical significance ($p < 0.05$, Table S-1). This may suggest that collisions occur randomly within the jars and that the mechanical energy may not consistently interact with the solid PFOA, resulting in variable outcomes across experimental runs.

Defluorination of over 80% of pure PFOA was observed with the addition of BN as a catalyst, for all milling times, on both our results and those presented by Yang *et al.* (2023)[25] (Fig. 1A). Our results showed a uniform defluorination trend with no increase over time confirmed by Analysis of Variance (ANOVA) and Tukey post hoc with no significant differences in defluorination efficiency among the 1-, 3-, and 4-hour treatments ($p > 0.05$, Table S-2). Notably, the 2-hour treatment yielded significantly higher defluorination, representing a 6–10% improvement compared to the other durations. This non-monotonic behavior suggests that the catalytic activity of BN may become depleted or less effective over time, limiting further degradation beyond the initial 80–90%. Yang *et al.* (2023) reported a similar trend, observing slightly lower efficiency after 4 hours of milling compared to 2 hours, although their efficiencies were nearly 10% higher than ours.[25] Additionally, as previously established, mechanical effects alone account for only ~1% defluorination, further reinforcing that prolonged milling without fresh catalyst input does not substantially enhance performance. The electric potentials generated by BN during ball impacts are likely responsible for the rapid mineralization of pure solid-phase PFAS within the ball milling system.

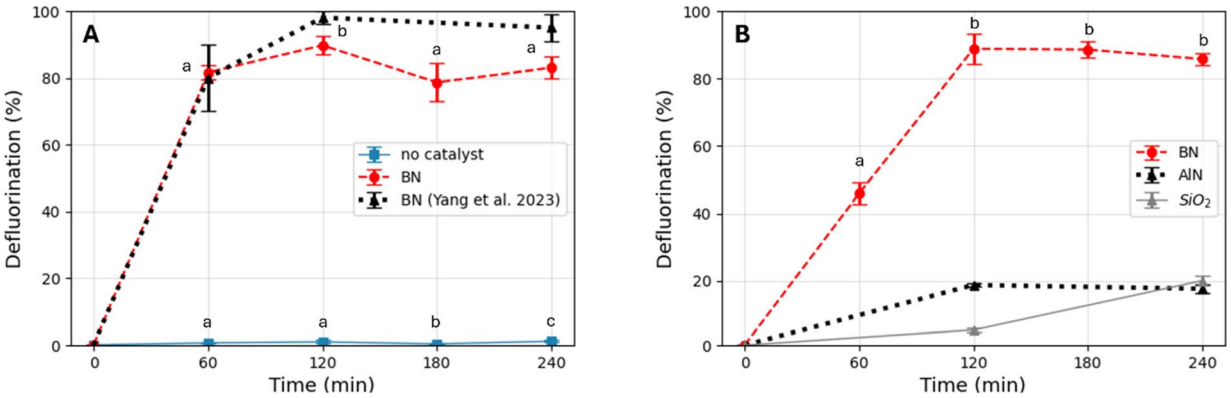

Fig. 1 Defluorination efficiency of PFOA under ball milling treatment, expressed as the percentage of measured fluoride ion relative to the total organic fluorine content of the initial PFOA. (A) Comparison of pure PFOA treated without a catalyst and with BN as a catalyst, based on results from this study and a previously published study. (B) Comparison of PFOA adsorbed onto activated carbon treated with three different catalysts. Different lowercase letters (a–c) indicate significant differences among milling times for the same treatment, at $p < 0.05$ (Tables S-1 to S-3).

When PFOA was adsorbed onto activated carbon, a clear linear increase in defluorination occurred between the 1-hour (46%) and 2-hour (89%) treatments (Fig. 1B), which contrasts with the behavior observed for pure PFOA. However, similar to the pure PFOA experiments, no further increase in defluorination efficiency was observed beyond the 2-hour treatment as ANOVA and Tukey post hoc tests revealed no significant differences among the 2-, 3-, and 4-hour treatments ($p > 0.05$, Table S-3). The lower defluorination observed at the 1-hour mark in the activated carbon experiments may be attributed to the physical distribution of PFOA: although the total mass of PFOA was kept constant, its dispersion across the porous matrix of the activated carbon likely diluted and spatially separated the molecules compared to the dense solid-phase form used in the pure PFOA trials. In this more dispersed form, the efficiency of the ball milling treatment appears more sensitive to treatment time, until, once again, the catalytic activity of BN diminishes after approximately 2 hours of milling.

Additional 2- and 4-hour tests were conducted using alternative catalysts, specifically aluminum nitride (AlN) and silicon dioxide (SiO_2), to explore potential substitutes for BN. However, both alternatives resulted in defluorination efficiencies of no more than 20% (Fig. 1B). These results are consistent with previous studies evaluating SiO_2 for pure PFAS compounds, which also reported defluorination below 20%.[24,28,32,33] Gobindlal *et al.*[32] suggested that the low efficiency could be attributed to the formation of unextractable fluorinated species and provided evidence from solid-state nuclear magnetic resonance (NMR) spectroscopy indicating the formation of insoluble Si–F bonds. These bonds likely hindered fluoride ion recovery during solvent extraction. We attribute the observed differences in catalytic efficiency primarily to the varying piezoelectric properties of the materials, specifically their piezoelectric strain coefficients under longitudinal mode activation (33-mode, d_{33}). Table 1 shows the d_{33} coefficients (in picocoulombs per newton, pC/N) for the three catalysts evaluated in this study, illustrating that BN exhibits a piezoelectric strain approximately 3.5 to 8 times higher than that of AlN and SiO_2, correlating well with the higher defluorination performance observed.

3.2. Sorption efficiency of activated carbon before and after ball milling

One of the key questions regarding the broader applicability of our ball milling system, particularly when used in combination with activated carbon for PFAS removal from potable water, was whether the activated carbon could be reused after treatment. Reusability would imply that the activated carbon could be recovered post-milling and retain sufficient sorption efficiency, which would lower overall treatment costs. We first evaluated the sorption performance of clean activated carbon and found it consistently adsorbed 98% of the 100 mg of PFOA tested (Fig. 2A). Although we were able to recover nearly all of the activated carbon after ball milling, its sorption capacity dropped to nearly 0% after 2 hours of treatment (Fig. 2A).

We further examine the activated carbon before and after treatment. The morphology of untreated activated carbon exhibits a rough surface with minimal deposition of fine particles, heterogeneous texture with prominent pits, elevations, and irregular contours—features that contribute to its porous structure and high surface area (Fig. 2B top). This morphology enables effective exposure of adsorption-active sites, which is critical for maintaining adsorption capacity, particularly for contaminants such as PFAS. In contrast, the ball-milled activated carbon displays a markedly altered morphology, with absence of the original pit-and-peak topography (Fig. 2B bottom). Instead, the surface is densely covered with fine particulates, likely occluding the pore structure and significantly reducing the accessible surface area. This observation is supported by the BET surface area analysis, where a nearly 50% reduction of surface area after ball milling was measured (Tables S-4 and S-5). This masking effect is believed to contribute to the reduced adsorption performance observed in subsequent treatment cycles.

The ball milling process was performed using stainless steel components, which typically contain iron (Fe), chromium (Cr),

Table 1 Piezoelectric strain coefficients (d_{33}) for each of the piezoelectric catalysts used

Piezoelectric material	d_{33} (pC/N) [source]	Max defluorination of PFOA in activated carbon[a]
BN	24.21 (ref. 34)	89%
AlN	5–7 (ref. 35)	19%
SiO_2	2–3 (ref. 36)	20%

[a] Maximum defluorination achieved after 2–4 hours of ball milling at a catalyst to PFOA ratio of 5 to 1.

and nickel (Ni). The presence of fine surface deposits in Fig. 2B (bottom) is likely caused by the abrasion of milling equipment, resulting in Fe, Cr, and Ni fragments embedding onto the activated carbon surface during processing. This is further supported by the EDS spectrum of untreated and treated activated carbon (Fig. 2C, and Tables S-6 and S-7), as well as the elemental mapping of the treated sample (Fig. S-2).

The EDS spectrum of the untreated control (Fig. 2C top) primarily displays peaks for C and O, the main components of activated carbon, along with minor peaks for S, Mg, Si, and Ca, likely from residual mineral debris. In contrast, the EDS spectrum of the ball-milled sample (Fig. 2C bottom) reveals a marked increase in Fe, Cr, and Ni content, alongside the original elements. Importantly, elemental mapping of the ball-milled sample (Fig. S-2), collected from the area shown in Fig. 2B (bottom), shows that fine particles containing Cr, Fe, and Ni are evenly distributed and closely correspond to the surface contours of the activated carbon, further indicating their origin from stainless steel abrasion during the milling process.

One potential approach to minimize the shedding of stainless steel particles during ball milling is to use jars and balls made from materials with higher surface hardness and therefore higher resistance to abrasion. Commercial options available for the ball milling system used in this study include zirconium oxide and tungsten carbide, both of which are significantly harder than stainless steel. Zirconium oxide approaches the hardness of advanced ceramics,[37] while tungsten carbide is among the hardest known materials, second only to diamond.[38] These alternatives are more expensive than

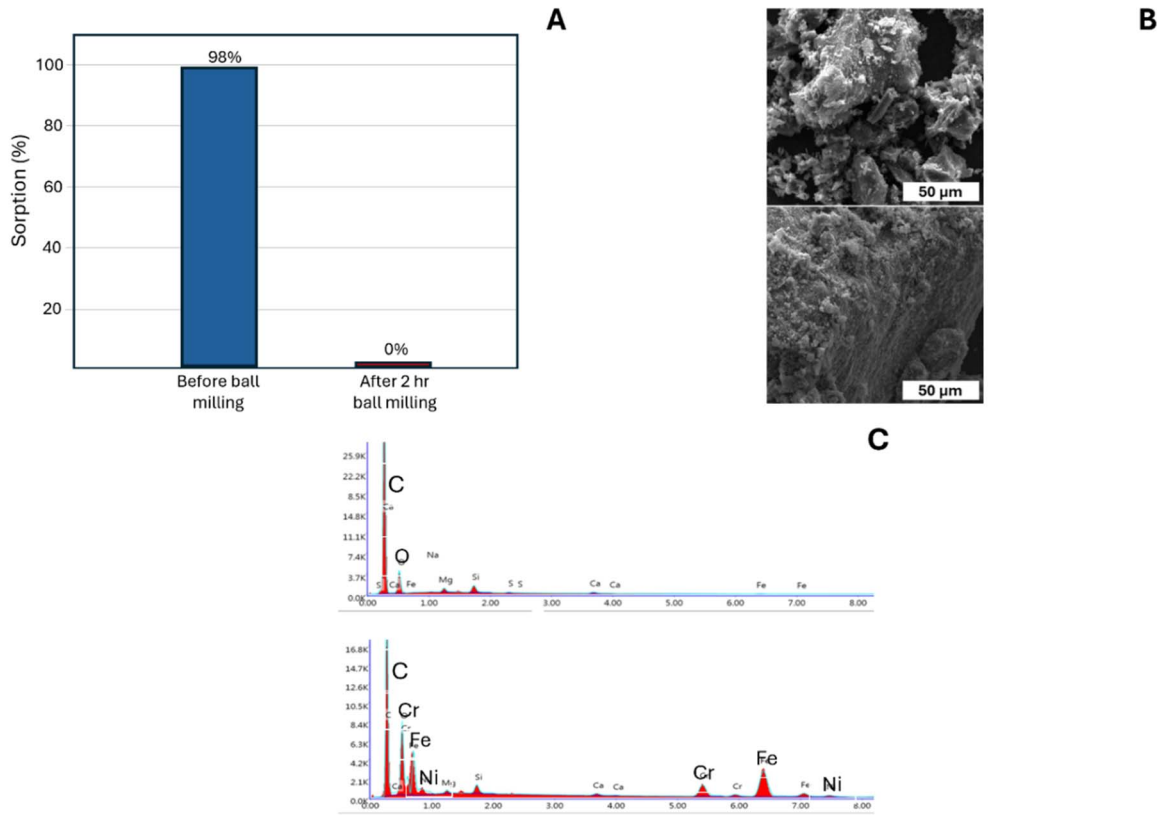

Fig. 2 Comparison of sorption efficiency and physical and chemical properties of activated carbon before and after ball milling. (A) Reduction in sorption efficiency after 2 hours of ball milling. (B) Change in surface area before (top) and after 2 hours of ball milling (bottom) seen with a scanning electron microscope. (C) Elemental analysis before (top) and after 2 hours of ball milling (bottom).

stainless steel. But future studies should evaluate whether using them could reduce the pore clogging on activated carbon, thereby increasing its potential for reuse in at least one additional adsorption cycle and potentially offsetting the higher upfront costs. However, even in the absence of material shedding, the high-energy ball impacts still deform the activated carbon structure, reducing pore space and overall surface area, which ultimately compromises its sorption performance.

At the 580 rpm used in our experiments, the impact force is approximately 57 N.[25] Reducing the speed to 500 rpm and 400 rpm lowers the force to about 45 N and 30 N, respectively, representing reductions of 21% and 47%.[25] While this suggests a gentler treatment, it raises the question of whether extended treatment times might still compromise the carbon's physical integrity. Reported evidence also suggests that prolonged milling, even at reduced speeds, can still degrade the surface area and porosity of activated carbon. For example, Yuan *et al.* (2023) showed that at 500 rpm, after 5 hours of milling the degradation notably increased with drops in surface area and porosity of 40% by 8 hours and more than 85% by 24 hours.[39] These findings may indicate that while lowering the milling intensity can reduce the immediate mechanical damage, extended milling durations needed to compensate for the lower energy input could still result in substantial degradation.

Even in the case of a one-time use of activated carbon, our methodology remains more cost-effective in the per-gram-of-PFAS basis than previously reported ball milling approaches. By leveraging the high sorption capacity of activated carbon, we successfully destroyed nearly 100 times higher mass of PFOA in less than one-third of the time compared to other studies that tested their defluorination in different media. For instance, prior studies showed that it required 6 to 10 hours of ball milling to destroy much smaller PFAS amounts, such as 93% of 0.3 mg in 2 g of sediment[25] or 90% of 9 mg in 1 mL of AFFF.[28] This demonstration highlights a scalable and efficient strategy for PFAS destruction, not only through the use of larger ball mills, but also by concentrating substantial PFAS loads into small amounts of activated carbon that can be processed with the same system described in this study.

3.3. Energy consumption and other considerations

The planetary ball mill used consumed approximately 0.14 kWh per hour. For a 2-hour treatment processing 400 mg of PFOA (100 mg per jar across four jars) or 4 g of activated carbon, this corresponds to an energy consumption of 0.7 kWh per gram of PFOA defluorinated, or 0.07 kWh per gram of activated carbon. In comparison with commercial technologies such as high-temperature incineration (TRL 9), which is currently the most widely used method for destroying PFAS adsorbed on activated carbon, the consumption of the ball mill is one order of magnitude higher, as incineration requires between 0.0031 and 0.0075 kWh per gram of activated carbon.[40] For a proof-of-concept technology like this (TRL 3–4), higher energy consumption is expected. While our approach demonstrates improved efficiency over previous ball milling experiments on a per-gram-of-PFAS basis due to the use of activated carbon, further optimization is necessary for it to be competitive at commercial scale.

One potential advantage over incineration, however, is that the ball milling reaction takes place in a sealed, enclosed environment, which inherently minimizes the risk of vapor-phase emissions during treatment, unlike incineration, where volatilization and atmospheric release are more likely. However, determining whether volatile short-chain PFAS were released upon opening the sealed jars after treatment was beyond the scope of this study, primarily due to the significant analytical challenges involved in reliably sampling and quantifying volatile fluorinated species in the post-milling headspace. We recommend that future studies consider this, or alternatively, analyze the total organic fluorine content in the rinsed water following milling, which indirectly may help estimate the fraction of fluorine potentially present in the gas phase.

4. Conclusions

This study demonstrates that while mechanical forces alone contribute minimally (~1%) to PFOA defluorination during ball milling, the addition of boron nitride (BN) as a catalyst significantly enhances PFAS degradation, achieving up to 90% mineralization within just two hours. However, the catalytic activity appears to plateau beyond this point, likely due to BN depletion and the random nature of ball collisions within the milling jars. When PFOA was adsorbed onto activated carbon, a slower but more predictable and time-dependent defluorination trend was observed, though similarly capped at around 90% after 2 hours. Importantly, while activated carbon proved highly effective in initially adsorbing PFOA, it lost nearly all sorption capacity following ball milling, indicating it cannot be reused for PFAS capture. Nonetheless, the ability to recover and safely mineralize nearly all PFAS from used activated carbon highlights the ball milling-BN system as a promising, and if it can be demonstrated that no volatile short-chain PFAS are released, potentially more environmentally sound strategy for the treatment and disposal of PFAS-contaminated materials.

Author contributions

Andres F. Prada: conceptualization, data curation, formal analysis, funding acquisition, project administration, writing – original draft. Jaemin Kim: conceptualization, funding acquisition. methodology, validation, writing – review and editing. Linduo Zhao: data curation, validation, visualization, writing – review and editing. Fangyu Li: data curation, formal analysis, methodology, writing – review and editing. Lee Green: data curation, resources, supervision. John W. Scott: conceptualization, funding acquisition, methodology, supervision, writing – review and editing.

Conflicts of interest

The authors declare that they have no known competing financial interests or personal relationships that could have appeared to influence the work reported in this paper.

Data availability

The data supporting this article have been included as part of the supplementary information (SI). Supplementary information: more details on the defluorination efficiencies, BET surface area analysis, and elemental composition of activated carbon before and after ball milling. See DOI: **https://doi.org/10.1039/d5mr00111k**.

Acknowledgements

This research was funded under the provisions of section 104 of the Water Resources Research Act annual base grants (104b) program made possible and distributed through the Illinois Water Resources Center and the U.S. Geological Survey, grant No. G21AP10618. Scanning electron microscopy (SEM) and energy-dispersive X-ray spectroscopy (EDS) were carried out in the Beckman Institute facilities at the University of Illinois. We thank Julissa Soto and Hannah Willey for their valuable assistance during the early stages of the laboratory work.

References

1 Z. Abunada, M. Y. D. Alazaiza and M. J. K. Bashir, An Overview of Per- and Polyfluoroalkyl Substances (PFAS) in the Environment: Source, Fate, Risk and Regulations, *Water*, 2020, **12**(12), 3590, DOI: **10.3390/w12123590**.

2 M. Lu, G. Cagnetta, K. Zhang, J. Huang and G. Yu, Mechanochemical mineralization of 'very persistent' fluorocarbon surfactants – 6:2 fluorotelomer sulfonate (6:2FTS) as an example, *Sci. Rep.*, 2017, **7**(1), 17180, DOI: **10.1038/s41598-017-17515-7**.

3 D. Ackerman Grunfeld, *et al.*, Underestimated burden of per- and polyfluoroalkyl substances in global surface waters and groundwaters, *Nat. Geosci.*, 2024, **17**(4), 340–346, DOI: **10.1038/s41561-024-01402-8**.

4 C. Gao, *et al.*, Factors Influencing Concentrations of PFAS in Drinking Water: Implications for Human Exposure, *ACS ES&T Water*, 2024, **4**(11), 4881–4892, DOI: **10.1021/acsestwater.4c00533**.

5 A. F. Prada, J. W. Scott, L. Green and T. J. Hoellein, Microplastics and per- and polyfluoroalkyl substances (PFAS) in landfill-wastewater treatment systems: A field study, *Sci. Total Environ.*, 2024, **954**, 176751, DOI: **10.1016/j.scitotenv.2024.176751**.

6 D. Huang, L. Yin and J. Niu, Photoinduced Hydrodefluorination Mechanisms of Perfluorooctanoic Acid by the SiC/Graphene Catalyst, *Environ. Sci. Technol.*, 2016, **50**(11), 5857–5863, DOI: **10.1021/acs.est.6b00652**.

7 J. W. Washington and T. M. Jenkins, Abiotic Hydrolysis of Fluorotelomer-Based Polymers as a Source of Perfluorocarboxylates at the Global Scale, *Environ. Sci. Technol.*, 2015, **49**(24), 14129–14135, DOI: **10.1021/acs.est.5b03686**.

8 I. Ross, *et al.*, A review of emerging technologies for remediation of PFASs, *Remed. J.*, 2018, **28**(2), 101–126, DOI: **10.1002/rem.21553**.

9 N. Merino, Y. Qu, R. A. Deeb, E. L. Hawley, M. R. Hoffmann and S. Mahendra, Degradation and Removal Methods for Perfluoroalkyl and Polyfluoroalkyl Substances in Water, *Environ. Eng. Sci.*, 2016, **33**(9), 615–649, DOI: **10.1089/ees.2016.0233**.

10 V. Franke, P. McCleaf, K. Lindegren and L. Ahrens, Efficient removal of per- and polyfluoroalkyl substances (PFASs) in drinking water treatment: nanofiltration combined with active carbon or anion exchange, *Environ. Sci.*, 2019, **5**(11), 1836–1843, DOI: **10.1039/C9EW00286C**.

11 S. J. Chow, *et al.*, Comparative investigation of PFAS adsorption onto activated carbon and anion exchange resins during long-term operation of a pilot treatment plant, *Water Res.*, 2022, **226**, 119198, DOI: **10.1016/j.watres.2022.119198**.

12 A. Malovanyy, *et al.*, Comparative study of per- and polyfluoroalkyl substances (PFAS) removal from landfill leachate, *J. Hazard. Mater.*, 2023, **460**, 132505, DOI: **10.1016/j.jhazmat.2023.132505**.

13 U.S. EPA, *Interim Guidance on the Destruction and Disposal of Perfluoroalkyl and Polyfluoroalkyl Substances and Materials Containing Perfluoroalkyl and Polyfluoroalkyl Substances*, 2024, accessed: Sep. 27, 2025, available: **https://www.epa.gov/system/files/documents/2024-04/2024-interim-guidance-on-pfas-destruction-and-disposal.pdf**.

14 F. Xiao, P. C. Sasi, A. Alinezhad, S. A. Golovko, M. Y. Golovko and A. Spoto, Thermal Decomposition of Anionic, Zwitterionic, and Cationic Polyfluoroalkyl Substances in Aqueous Film-Forming Foams, *Environ. Sci. Technol.*, 2021, **55**(14), 9885–9894, DOI: **10.1021/acs.est.1c02125**.

15 J. Wang, *et al.*, Critical Review of Thermal Decomposition of Per- and Polyfluoroalkyl Substances: Mechanisms and Implications for Thermal Treatment Processes, *Environ. Sci. Technol.*, 2022, **56**(9), 5355–5370, DOI: **10.1021/acs.est.2c02251**.

16 U.S. Department of Defense, *Memorandum for Incineration Prohibition Policy Update*, Washington, DC, 2023, accessed: Jul. 01, 2025, available: **https://www.acq.osd.mil/eie/eer/ecc/pfas/docs/news/Memorandum-for-Incineration-Prohibition-Policy-Update.pdf**.

17 M. J. Krause, *et al.*, Supercritical Water Oxidation as an Innovative Technology for PFAS Destruction, *J. Environ. Eng.*, 2022, **148**(2), 05021006, DOI: **10.1061/(ASCE)EE.1943-7870.0001957**.

18 B. D. Fennell, S. Chavez and G. McKay, Destruction of Per- and Polyfluoroalkyl Substances in Reverse Osmosis Concentrate Using UV-Advanced Reduction Processes, *ACS ES&T Water*, 2024, **4**(11), 4818–4827, DOI: **10.1021/acsestwater.4c00458**.

19 D. Palma, *et al.*, PFAS Degradation in Ultrapure and Groundwater Using Non-Thermal Plasma, *Molecules*, 2021, **26**(4), 924, DOI: **10.3390/molecules26040924**.

20 S. Hao, Y.-J. Choi, B. Wu, C. P. Higgins, R. Deeb and T. J. Strathmann, Hydrothermal Alkaline Treatment for Destruction of Per- and Polyfluoroalkyl Substances in Aqueous Film-Forming Foam, *Environ. Sci. Technol.*, 2021, **55**(5), 3283–3295, DOI: **10.1021/acs.est.0c06906**.

21 A. Yanagida, E. Webb, C. E. Harris, M. Christenson and S. Comfort, Using Electrochemical Oxidation to Remove PFAS in Simulated Investigation-Derived Waste (IDW): Laboratory and Pilot-Scale Experiments, *Water*, 2022, **14**(17), 2708, DOI: 10.3390/w14172708.
22 G. Cagnetta, J. Huang, B. Wang, S. Deng and G. Yu, A comprehensive kinetic model for mechanochemical destruction of persistent organic pollutants, *Chem. Eng. J.*, 2016, **291**, 30–38, DOI: 10.1016/j.cej.2016.01.079.
23 N. Bolan, *et al.*, Remediation of poly- and perfluoroalkyl substances (PFAS) contaminated soils – To mobilize or to immobilize or to degrade?, *J. Hazard. Mater.*, 2021, **401**, 123892, DOI: 10.1016/j.jhazmat.2020.123892.
24 K. Zhang, J. Huang, G. Yu, Q. Zhang, S. Deng and B. Wang, Destruction of Perfluorooctane Sulfonate (PFOS) and Perfluorooctanoic Acid (PFOA) by Ball Milling, *Environ. Sci. Technol.*, 2013, **47**(12), 6471–6477, DOI: 10.1021/es400346n.
25 N. Yang, *et al.*, Solvent-Free Nonthermal Destruction of PFAS Chemicals and PFAS in Sediment by Piezoelectric Ball Milling, *Environ. Sci. Technol. Lett.*, 2023, **10**(2), 198–203, DOI: 10.1021/acs.estlett.2c00902.
26 L. Duan, *et al.*, Efficient Photocatalytic PFOA Degradation over Boron Nitride, *Environ. Sci. Technol. Lett.*, 2020, **7**(8), 613–619, DOI: 10.1021/acs.estlett.0c00434.
27 J. Zhu, N. Yang, S. Fernando, A. Rossner, T. M. Holsen and Y. Yang, Piezoelectric Ball Milling Treatment of PFAS-Laden Spent Resins, *Environ. Sci. Technol. Lett.*, 2025, **12**(4), 461–466, DOI: 10.1021/acs.estlett.5c00196.
28 N. Yang, *et al.*, PFAS Destruction and Near-Complete Defluorination of Undiluted Aqueous Film-Forming Foams at Ambient Conditions by Piezoelectric Ball Milling, *Environ. Sci. Technol.*, 2025, **59**(3), 1854–1863, DOI: 10.1021/acs.est.4c07906.
29 D. Li, *et al.*, Efficient removal of short-chain and long-chain PFAS by cationic nanocellulose, *J. Mater. Chem. A*, 2023, **11**(18), 9868–9883, DOI: 10.1039/D3TA01851B.
30 X. Huang, *et al.*, Comparison of perfluoroalkyl substance adsorption performance by inorganic and organic silicon modified activated carbon, *Water Res.*, 2024, **260**, 121919, DOI: 10.1016/j.watres.2024.121919.
31 S. J. Smith, M. Lauria, C. P. Higgins, K. D. Pennell, J. Blotevogel and H. P. H. Arp, The Need to Include a Fluorine Mass Balance in the Development of Effective Technologies for PFAS Destruction, *Environ. Sci. Technol.*, 2024, **58**(6), 2587–2590, DOI: 10.1021/acs.est.3c10617.
32 K. Gobindlal, Z. Zujovic, J. Jaine, C. C. Weber and J. Sperry, Solvent-Free, Ambient Temperature and Pressure Destruction of Perfluorosulfonic Acids under Mechanochemical Conditions: Degradation Intermediates and Fluorine Fate, *Environ. Sci. Technol.*, 2023, **57**(1), 277–285, DOI: 10.1021/acs.est.2c06673.
33 L. P. Turner, *et al.*, Mechanochemical remediation of perfluorooctanesulfonic acid (PFOS) and perfluorooctanoic acid (PFOA) amended sand and aqueous film-forming foam (AFFF) impacted soil by planetary ball milling, *Sci. Total Environ.*, 2021, **765**, 142722, DOI: 10.1016/j.scitotenv.2020.142722.
34 M. Noor-A-Alam and M. Nolan, Engineering Ferroelectricity and Large Piezoelectricity in h-BN, *ACS Appl. Mater. Interfaces*, 2023, **15**(36), 42737–42745, DOI: 10.1021/acsami.3c07744.
35 K. Hirata, H. Yamada, M. Uehara, S. A. Anggraini and M. Akiyama, First-Principles Study of Piezoelectric Properties and Bonding Analysis in (Mg, X, Al)N Solid Solutions (X = Nb, Ti, Zr, Hf), *ACS Omega*, 2019, **4**(12), 15081–15086, DOI: 10.1021/acsomega.9b01912.
36 M. Liu, *et al.*, Measurement of Longitudinal Piezoelectric Coefficients (d33) of Pb(Zr0.50,Ti0.50)O3 Thin Films with Atomic Force Microscopy, in *3rd International Symposium on Instrumentation Science and Technology*, Xi'an., China, 2004, pp. 352–356.
37 M. K. Mohammed, A. Alahmari, H. Alkhalefah and M. H. Abidi, Evaluation of zirconia ceramics fabricated through DLP 3d printing process for dental applications, *Heliyon*, 2024, **10**(17), e36725, DOI: 10.1016/j.heliyon.2024.e36725.
38 A. S. Kurlov and A. I. Gusev, *Tungsten Carbides*, Springer International Publishing, Cham, 2013, vol. 184, DOI: 10.1007/978-3-319-00524-9.
39 R. Yuan, *et al.*, Structural transformation of porous and disordered carbon during ball-milling, *Chem. Eng. J.*, 2023, **454**, 140418, DOI: 10.1016/j.cej.2022.140418.
40 A. L. Ling, *et al.*, Spent Media Management Pathways for PFAS Treatment Applications, *Water Environ. Res.*, 2025, **97**(7), e70130, DOI: 10.1002/wer.70130.